Adsorption Performance of Packed Bed Column for the Removal of Lead (II) using Velvet Tamarind (*Dialium indum*) Shells

Abstract

The removal of Pb ions by activated carbons prepared from velvet tamarind (Dialium indum) shells was studied to investigate its uptake potentials using column sorption at different operating conditions (flow rates ,initial concentrations and bed height). The prepared adsorbent was characterized by determining the physicochemical properties, proximate analysis, carbon, Hydrogen, Nitrogen and Sulpur analysis, Fourier Transform-Infra Red, Potentiometric titration. Different dynamic models were used to describe the sorption processes. The FTIR analysis results suggested the presence of functional groups such as hydroxyl, carbonyl, carboxyl and amine which could bind the metals and remove them from the solution. The values of moisture content, volatile matter, fixed carbon and ash content as obtained from % proximate analysis are 3.43, 27.07, 65.05, 4.45 for activated carbons prepared from velvet tamarind shells. Ultimate analysis revealed that activated carbons prepared from velvet tamarind shells contained 75% carbon. The surface area and Iodine number of activated carbon from velvet tamarind shell are 570 m^2g^{-1} and 614.7 mgg^{-1} respectively. The column experimental data revealed that an increase in bed height and initial metal concentration or a decrease of flow rate enhances the longevity of column performance by increasing both breakthrough time and exhaustion time thereby delaying bed saturation. Low ash content and high surface areas are indication of good mechanical strength and microporosity of the activated carbons prepared from this precursor. The activated carbons are inexpensive and appeared to be effective and can be explore for future commercial application for environmental sustainability.

Key words: Adsorbent; velvet tamarind; adsorption; Pollution;

1. INTRODUCTION

The exponetial increase in the world population as well as increase in industrial activities made environmental pollution an important issue of serious concern. Gaseous, liquid and solid wastes emanates from these activities. Earth's surface is made up of 70% water which is the most valuable natural resource existing on our planet without which life becomes impossible. Although this fact is widely recognized, pollution of water resources is a common problem being faced today. Lakes, rivers and oceans are being overwhelmed with many toxic contaminants [1].

Among toxic substances exceeding threshold levels are heavy metals and water pollution by heavy metals occurs directly by effluent discharge from industries such as textiles, dyes, leather tanning, electroplating, metal finishing, refineries, mine water and waste treatment plants and indirectly by the contaminants that enter the water supply from soils/ground water systems and from the atmosphere via rain water. The presence of these toxic substances in an undesirable level in wastewaters makes their removal to receive much attention [2]. When heavy metal concentration in waste water is considerably high, it would endanger public health and the environment if discharged into the environment without adequate treatment [3].

Several methods such as ion exchange, solvent extraction, reverse osmosis, and precipitation have been used for the removal of heavy metals from aqueous solutions but most of these methods are non-economical and have many

disadvantages such as high reagents and energy requirements, generation of toxic sludge of other waste products that also require disposal after treatment [4]. However, adsorption of heavy metals from aqueous solutions is a well established process that has proven very efficient and promising in the removal of contaminants from aqueous effluents where interactions between metal ions and biomass present potential applications for the remediation of metal contaminated waters in various industries [3]. The process of adsorption has an edge over other methods due to its sludge free clean operation and efficient removal of toxic metals even from dilute solution. It is as an innovative principle of using waste to treat waste and will be more efficient because the agricultural by-products used as adsorbents are readily available, affordable, eco-friendly and have high uptake capacity for heavy metals due to the presence of functional groups which can bind metals to effect their removal from effluents making it more cost effective than the use of commercial activated carbon which is expensive. Alternative activated carbon produced from velvet tamarind fruits will be cheap, locally available and could be used to reduce environmental pollution by heavy metals.

The release of toxic metals into the environment would be controlled in this way, and so, the process could be used more extensively as an alternative method to the conventional treatment techniques [5].

Considerable attention has been devoted to the development of unconventional materials like used agricultural by-products for the removal of heavy metals from waste water [6], since these plant based by-products represent waste resources, and are widely available and environmentally friendly [7]. Various natural adsorbents obtained from agricultural wastes like sun flower stalk, Eucalyptus bark, maize husk, coconut shell, waste tea, rice straw, tree leaves, peanut and walnut husk, palm fruit bunch and African spinach stalk have been tried as raw materials for adsorbents to achieve effective removal of various heavy metals[8][9].

Commercial activated carbons have been used for the removal of heavy metals but are imported and expensive. There is a need to look for viable non-conventional low-cost adsorbents as alternative to commercial activated carbon in order to meet the growing demand for cheaper and effective adsorbents. Velvet tamarind is among common fruits produced in Nigeria and large volumes of its non-edible and non useful parts such as the shells constitute environmental problems. These non essential parts of velvet tamarind could be explored for the production of activated carbon.

The aim of this study is to prepare, characterize and assess the heavy metal adsorption potentials of activated carbons produced from velvet tamarind.

2. Materials and Methods

2.1 Sample Collection and Preparation

The carbonaceous precursor used for preparation of activated carbon is velvet tamarind shells that were obtained as agricultural and forest wastes. Prior to use, samples were washed gently with water to remove mud and other impurities present on the surface and then sundried for one week. The samples shells collected after discarding the fruit pulp, were washed with deionized water, sun dried and then dried in a vacuum oven at 80^{o}C for 24 h, crushed and ground using mortar and pestle. The particles were separated by using a US standard testing sieve (No. 100~No. 200). 100 g of raw

material was impregnated with 100 cm^3 of concentrated H_2SO_4 for 12 h. The impregnation was carried out at 70 ^oC in a hot air oven to achieve well penetration of chemical into the interior of the precursor. The sieved samples were placed in a crucible and heated in a muffle furnace for 60 min at 500^oC. Activated carbons produced were cooled in desiccators and rinsed with deionized water until neutral pH was attained and stocked for subsequent heavy metal removal tests and analysis.

2.2 Sample Characterization

The pH, bulk density, iodine number, specific surface area, chemical composition of the adsorbents, proximate analysis of the activated carbons were determined using standard test [10][11][12][13]. Ultimate analysis (CHNS elemental analysis) of the samples were determined by subjecting them to combustion process (furnace at ca. 1000^oC) for 30 min, where carbon was converted to carbon dioxide; hydrogen to water; nitrogen to nitrogen gas/ oxides of nitrogen and sulphur to sulphur dioxide. The combustion products were swept out of the combustion chamber by inert carrier gas and passed over heated (about 600^o C) high purity copper situated at the base of the combustion chamber to remove any oxygen not consumed in the initial combustion and to convert any oxides of nitrogen to nitrogen gas. The gases were then passed through the absorbent traps in order to leave carbon dioxide, water, nitrogen and sulphur dioxide which were separated and detected using GC and thermal conductivity detection.

2.3 Fourier Transform Infrared (FTIR) Spectrometer

FTIR analysis was made using IPRrestige-21, FTIR-84005, SHIMADZU Corporation (Kyoto, Japan). Sample of 0.1 g was mixed with 1 g of KBr, spectroscopy grade (Merk, Darmstadt, Germany), in a mortar. Part of this mix was introduced in a cell connected to a piston of a hydraulic pump giving a compression pressure of 15 kPa / cm^2. The mix was converted to a solid disc which was placed in an oven at 105^oC for 4 h to prevent any interference with any existing water vapor or carbon dioxide molecules. Then it was transferred to the FTIR analyzer and a corresponding spectrum was obtained showing the wave lengths of the different functional groups in the sample which were identified by comparing these values with those in the library.

2.4 Preparation of Pb Solution (Simulated Effluent)

Standard lead (Pb) stock solution (1000 $mgdm^{-3}$) was prepared by placing 1.578 g $Pb(NO_3)_{2,}$ in a volumetric flasks to which 100 cm^3 of deionized water was added. The flasks were shaken vigorously to ensure the dissolution of the mixture. The solution was made up to 1000 cm^3 mark with deionized water. The working concentrations were prepared from the stock solution by serial dilution. pH adjustment of solutions were made using dilute NaOH and HCl solutions. Deionized water was used to prepare all the solutions. All reagents were of analytical grade.

2.5 Fixed Bed Column Experimental Procedure

Fixed bed column studies were carried out using a glass column of 30 mm internal diameter and 400 mm length. The activated carbon having 0.425 to 0.600 mm particle size range was used. The activated carbon was packed in the column with a layer of glass wool at the top and bottom. Bed height of 50, 100 and 150 mm were used. The tank containing the heavy metal solution was placed at a higher elevation so that the metal solution could be introduced into the column by gravitational flow. The flow controller helps to regulate the flow rate. Three flow rates (1, 3 and 5 cm^3min^{-1}) were used while initial ion concentrations of 50, 100 and 150 $mgdm^{-3}$ were used. The effluent samples were collected at hourly intervals and analyzed for the residual metal concentration using atomic absorption spectrophotometer.

2.6 Dynamic models of Column Adsorption of lead (Pb) onto activated carbon from Velvet Tamarind (*Dialium indum*) Shells

For the successful design of a column adsorption process, it is important to predict the concentration-time profile or breakthrough curve for effluent parameters. A number of mathematical models have been developed for use in the design of continuous fixed bed sorption columns. In this work, the Bed Depth Service Time (BDST), Thomas and Yoon-Nelson models were used in predicting the behavior of the breakthrough curve because of their effectiveness. The model's equations are presented in Equations 1 to 3:

BDST = $t = \frac{No}{CoF}Z - \frac{1}{KaCo}\ln\left(\frac{Co}{CB}\right) - 1$ (1)

Thomas = $\ln\left(\frac{Co}{Ct} - 1\right) = \frac{KthqoM}{Q} - KthCot$ (2)

Yoon-Nelson = $\ln\left(\frac{Ct}{Co-Ct}\right) = Kynt - \tau Kyn$ (3)

The maximum column capacity, q_{total} (mg) for a bed height of 10.00 cm, initial metal concentration of 50.00 mg/dm^3 and flow rates of 1, 3 and 5 cm^3min^{-1} was calculated from the area under the breakthrough curves as given by the Equation 4 (Ahmad and Hameed, 2010)

$$q_{total} = \frac{QA}{1000} = \frac{Q}{1000}\int_{t=0}^{t=total} Cad\, dt \quad (4)$$

where $Cad = Ci - Ce$ (mg L^{-1}), $t = total$ is the total flow time (min), Q is the flow rate (cm min^{-1}) and A is the area under the breakthrough curve (cm^2).

The equilibrium uptake ($qe_{(exp)}$), i.e. the amount of the metals adsorbed (mg) per unit dry weight of adsorbent (mgg^{-1}) in the column, was calculated from Equation 5 (Martin-Lara *et al*., 2012):

$$qe_{(exp)} = \frac{qtotal}{W} \quad (5)$$

where W is the total dry weight of velvet tamarind shell in the column (g)

The total volume treated, V_{eff} (cm^3) was calculated from Equation 6 (Futalan *et al*., 2011)

$$V_{eff} = Qt_{total} \quad (6)$$

The mass transfer zone (Zm) is one of the widely used parameters to examine the effects of the column adsorption height. To determine the length of the adsorbent zone in the column, Zm was calculated from Equation 7:

$$Zm(cm) = Z(t_e - t_b/t_e) \quad (7)$$

where, L presents the closed height (cm), t_b is the time (minute) required to reach the breakthrough point or C_{eff}/Co = 0.05 and t_e is the time (minute) required to reach the exhaustion point or C_{eff}/Co = 0.95 (Apiratikul and Pavasant, 2008).

3.0 RESULTS AND DISCUSSION

The proximate analysis, ultimate analysis and physicochemical properties of activated carbons produced from velvet tamarind shells are presented in Tables 1, 2 and 3

Table 1. Proximate analysis, of the activated carbons prepared from velvet tamarind shells

Property	Vt
Moisture	3.43
Volatile Matter	27.07
Fixed carbon	65.05
Ash	4.45

Vt = activated carbon from velvet tamarind fruit shells

3.0 Ultimate Analysis of Activated Carbons from Velvet Tamarind Fruit Shells

Element	Vt
C	75
H	1.2
N	1.8
S	0.8
O	21.5

Table 2. Physicochemical Properties of Activated carbons prepared from Velvet Tamarind shells.

Parameter	Vt
Bulk density (gcm^{-3})	0.51
Iodine number (mgg^{-1})	614.7
Surface area (m^{2}g^{-1})	570
Particle density (gcm^{-3})	0.72
Porosity (%)	26.4
pH	6.9
Pore Volume	0.13

3.1 Proximate and ultimate analysis of activated carbons from velvet tamarind shells

According to [14], ash content is the measurement of the amount of mineral (e.g. Ca, Mg, Si and Fe) in activated carbon. Ash content obtained in this work was 4.45 for activated carbons prepared from velvet tamarind shells (Table 1). The ash content of this carbon is well below the typical ash content values of 8-12% obtained by [15] and 12% obtained by [16] but higher than the 3.58 and 4.89 obtained by [17] and [18] for coconut and Bael fruit shell respectively. Typical ash content of activated carbons is around 5-6 % [19]. A small increase in ash content causes a decrease in adsorptive properties of activated carbons by reducing the mechanical strength of carbon and affects adsorptive capacity. The presence of ash has been shown to inhibit surface development [20].

The value of 78 and 65.05% fixed carbon were obtained from percentage ultimate and proximate analysis of activated carbon prepared from velvet tamarind fruit shells (Table 1&2). [21] prepared activated carbon from *Euphorbia antiquorum* and obtained 57.94% fixed carbon. [22] reported values ranging from 23.7 to 87.13% within 450 to 950^{o}C. Carbonization leads to carbon atoms rearrangement into graphitic-like structures and the pyrolytic decomposition of the precursor and non-carbon species elimination, resulting in a fixed carbonaceous char produced [23]. Also activating agents act as dehydrating agents and oxidants which also influence the pyrolytic decomposition and prevent the formation of the tar or ash, hence developing the carbon yield. The combine influence of activation and carbonization increases carbon yield.

As reported in Table 3.0, the following; 0.51 g/cm^3, 614.7 mg/g, 570 m^2/g, 26.4% were obtained as the values of bulk density, iodine number, surface area and porosity for activated carbon prepared from Velvet Tamarind shells. The values of bulk density, surface area, and iodine number were similar to the values obtained by [24][26] produced

activated carbon from palm kernel shell and obtained yields of bulk density of 0.5048g/cm^3, iodine number of 766.99 mgg^{-1} and 669.75 m^{2}g^{-1} BET surface area. Bulk density is the weight per unit volume of dry carbon in a packed bed and is 80-85% of the apparent density [27]. Higher density provides greater volume activity and normally indicates better quality activated carbon. [28] in his comparative adsorption studies for the removal of copper (II) from aqueous solution by different adsorbent obtained bulk density values ranging from 0.32 to 0.62 gcm^{-3}. Bulk density of 0.48 gcm^{-3} was obtained by [21] and is lower than 0.51 gcm^{-2} obtained for velvet tamarind shells.

The iodine number value is an indication of surface area of the activated carbon [29]. Activated carbons with iodine numbers of about 550 mgg^{-1} can be attractive for waste water treatment from the user's viewpoint [30]. The iodine number values of 614.7 mgg^{-1} was obtained for activated carbon prepared from velvet tamarind fruits shells (Table 3.0). These results were within the range of 608 and 746 mgg-1 obtained by [31]. Analysing the iodine number of activated carbon prepared from palm-oil shell by pyrolysis and steam activation in a fixed bed reactor, [25] obtained maximum value of 766.99 mgg^{-1} at 750^{o}C. According to [13], each 1.0mg of iodine adsorbed is ideally considered to represent 1.0 m^2 of activated carbon internal area. Therefore the adsorbents have enough internal surface area for adsorption.

3.2 Surface area of activated carbons from velvet tamarind fruit shells

Surface area is the carbon particle area available for adsorption. In general, the larger the effective surface area, the greater is the adsorption capacity. A surface area of the activated carbons used in this study is as reported in Table 4.0. The results indicated that the surface area of 570 m^{2}g^{-1} was obtained for velvet tamarind shells activated carbon. The specific surface area as indicated in Table 4.0 further confirmed the porous nature of the activated carbons. According to [32], an adsorbent with a surface area of 500 m^{2}g^{-1} and above has a well formed microporous structures suitable for adsorption. According to [31], 95% of the total surface areas of a given adsorbent are micropores. [33] stated that most widely used commercial activated carbon has surface areas of between 600-1000 m^{2}g^{-1}.

3.3 pH of activated carbons from velvet tamarind fruit shells

The pH of activated carbon can be defined as the pH of a suspension of carbon in distilled water. The chemical nature of the carbon surfaces are mostly deduced from the acidity or pH of the carbon. Table 4.0 presented the pH of the activated carbon prepared from velvet tamarind fruits shells as 6.9. The results suggest weakly acidic surface properties. Similar results were obtained by [34]. [20] obtained pH between 6.4 and 7.4 for activated carbon prepared from bagasse.

3.4 Moisture content of activated carbons from velvet tamarind shells

Moisture content was measured from loss of water over initial weight of raw materials. Usually moisture content decreases as the temperature increases. As presented in Table 4.0, moisture content of 3.43% was obtained for the activated carbon prepared from Velvet tamarind fruits shells. [25] obtained values between 8.35 to 11.38% for moisture content while [16] obtained 4.33% in their work. The moisture contents of commercial activated carbons ranged between 2- 10 % [33]. The practical limit for the level of moisture content allowed in the activated carbon varies within 3 to 6% [6]. The moisture content of 3.43% obtained for the the activated carbon prepared from Velvet tamarind fruits shells activated carbons therefore fall within the practical limit.

3.5 Volatile matter of activated carbons from velvet tamarind shells

The values of volatile matter of 27.07% (Table 1.0) was obtained for Velvet tamarind fruit shells activated carbons. Lou *et al.* (1999) studied chars prepared from oil palm waste and obtained % volatile matter ranging from 74.86 to 4.08% between 450 to 950^{o}C.

3.6 Potentiometric titration curves of activated carbons from velvet tamarind fruit shells

Figures 1.0 indicate the result of potentiometric curves of the activated carbons investigated to determine the Point of Zero Charge on the surface of the adsorbent. The point of zero charge (PZC) is an adsorption phenomenon which describes the condition when the electrical charge density on a surface is zero. The common intersection point of the titration curves with the blank is the pH at PZC (pH_{PZC}). From the curves (Figure 1.0), the pH_{PZC} for activated carbon prepared from velvet tamarind shells were identified as 5.50.

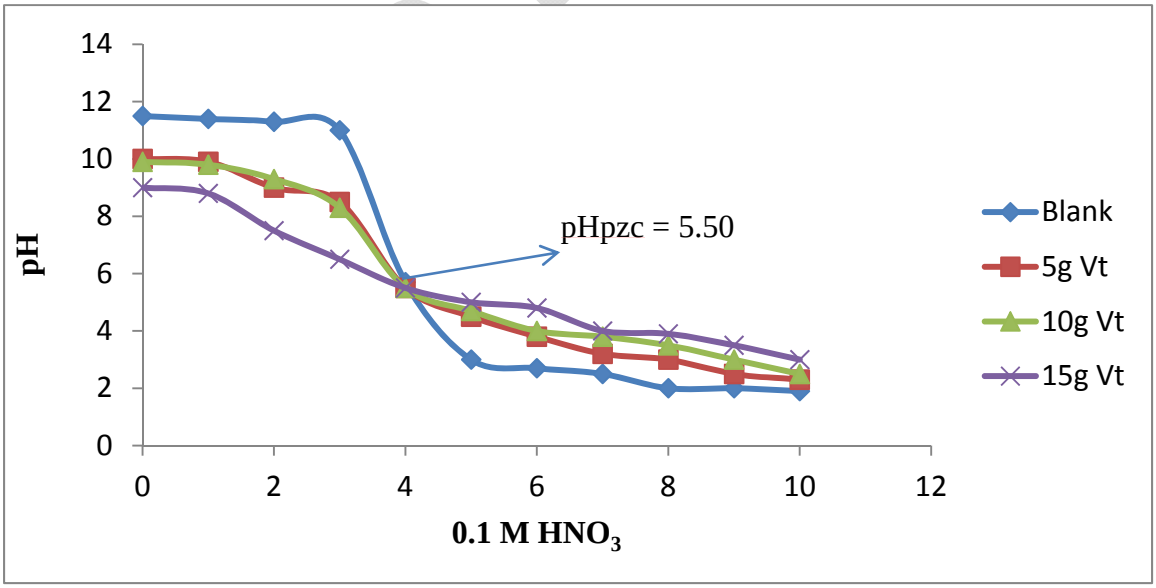

Figure 1.0: Potentiometric Titration Curves of Activated Carbon from Velvet Tamarind Shell

The titration curve of Velvet tamarind shells is a bit steep. This indicates a moderate capacity of the shells to take up protons (buffering capacity). Therefore, the capacity to take up cationic metals by ionic exchange is probably also moderate. Any pH above pH(pzc) provide a negatively charged surface favourable for adsorption of cationic heavy metals from the solution.

3.7 Fourier transforms infrared spectrometer (FTIR) result of activated carbons from velvet tamarind

The FTIR spectral of activated carbons prepared from velvet tamarind fruit shells were used to determine the vibration frequency changes in the functional groups on the surface which facilitates the adsorption of metal ions. The spectra of the activated carbons were measured within the range of 400 – 4000cm^{-1} wave number as shown in Figures 2.0.

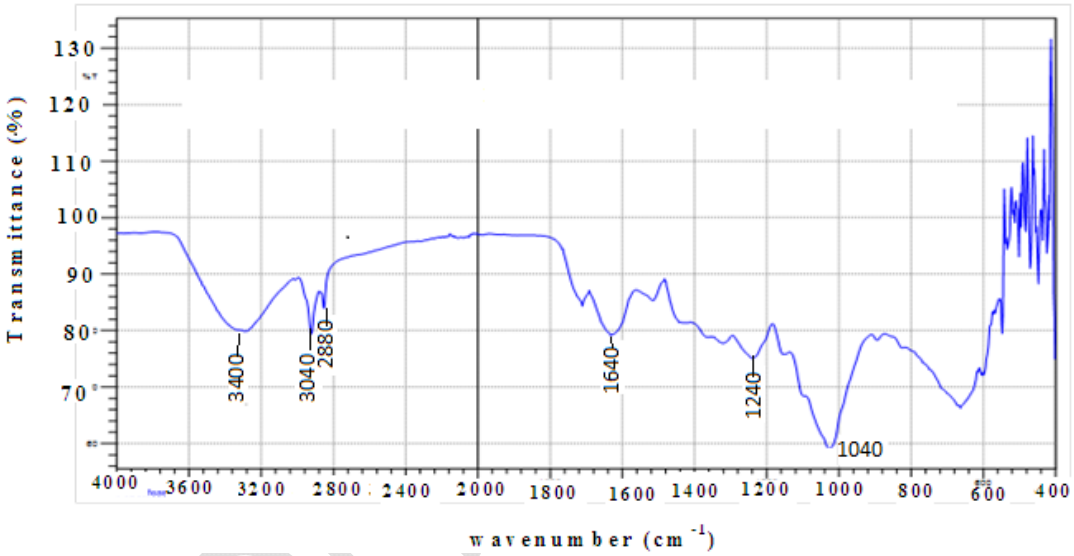

Figure 2.0: FTIR Spectrum of Activated carbon prepared from Velvet Tamarind Shell

The FTIR analysis result (Figure 2.0) suggest the presence of such functional groups as the carboxylic acid or alcoholic O-H bond stretching which may overlap with amine (N-H) bond stretching at peaks between 3250-3400 cm^{-1}; possible C=O bond of carbonyl or amide groups within 1640-1670 cm^{-1}; C-O and O-H bond stretching of alcohol and ethers at 1000-1260 cm^{-1} of the finger-print region (Gimba et al, 2001). The important parameters that influence and determine the adsorption of metal ions from aqueous solutions are the carbon-oxygen functional groups present on the carbon surface and the pH of the solution (Bansal and Goyal, 2005).

3.8 Column Adsorption Studies of Lead (Pb) on Activated carbon Prepared from Velvet Tamarind Shells

3.8.1 Effect of bed height

The adsorption of metal ions in the packed bed column is largely dependent on the bed height, which is directly proportional to the quantity of adsorbent in the column. The effect of bed height on breakthrough curve analysis was studied by varying the bed height from 5 cm to 15 cm at increment of 5cm. The adsorption breakthrough curves were obtained by varying the bed heights at a flow rate of 1cm^3/min and an inlet Pb ions concentration of 50 mg/dm^3. The breakthrough curves are presented in Figures 2.0. Faster breakthrough curves were observed for a bed height of 5 cm compared to the bed height of 10 cm and 15 cm.

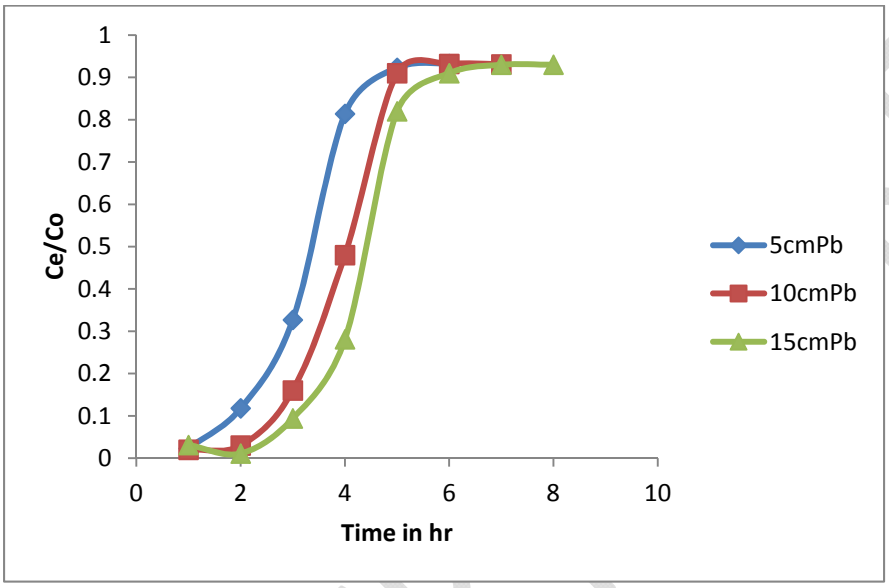

Figure 3.0: Column adsorption of Pb(II) by Activated Carbon from Velvet Tamarind Fruits Shells at different Bed height

As depicted by Figure 3.0, the breakthrough time varied with bed height. Steeper breakthrough curves were achieved with a decrease in bed depth. The breakthrough time decreased with a decreasing bed depth from 15 to 5 cm, as binding sites were restricted at low bed depths. At low bed depth, the metal ions do not have enough time to diffuse into the surface of the adsorbents, and a reduction in breakthrough time occurs. Conversely, with an increase in bed depth, the residence time of metal ions solution inside the column was increased, allowing the metal ions to diffuse deeper into the adsorbents.

The results indicate that the throughput volume of the aqueous solution increased with increase in bed height, due to the availability of more number of sorption sites [21]. At higher bed depth of 10 cm, adsorbent mass was more residing in the column thereby providing larger service area for binding, fixation, diffusion and permeation of the solute to the

adsorbent. Longer bed depth also provided more reaction area and larger volume of influent treatment which translated to higher adsorption capacity.

The equilibrium sorption capacity decreased with increase in bed height. This shows that at smaller bed height, the effluent adsorbate concentration ratio increased more rapidly than for a higher bed height. Furthermore, the bed is saturated in less time for smaller bed heights. The slope of the S-shape from t_b to t_e decreased as the bed height increased from 5 to 15 cm, indicating the breakthrough curve becomes steeper as the bed height decreased. Also the breakthrough time (t_b) and exhaustion time (t_e) increase with increase in bed depth

3.8.2 Effect of Initial Metal Concentration

A Series of column experiments with different metals concentrations namely, 50, 100 and 150 ppm were conducted to investigate the effect of initial metal concentration on the performance of the fixed-bed operation. Figure 3.0 presented the breakthrough curves for the adsorption of Pb onto Velvet tamarind fruit shells activated carbon at various initial metal concentrations.

.

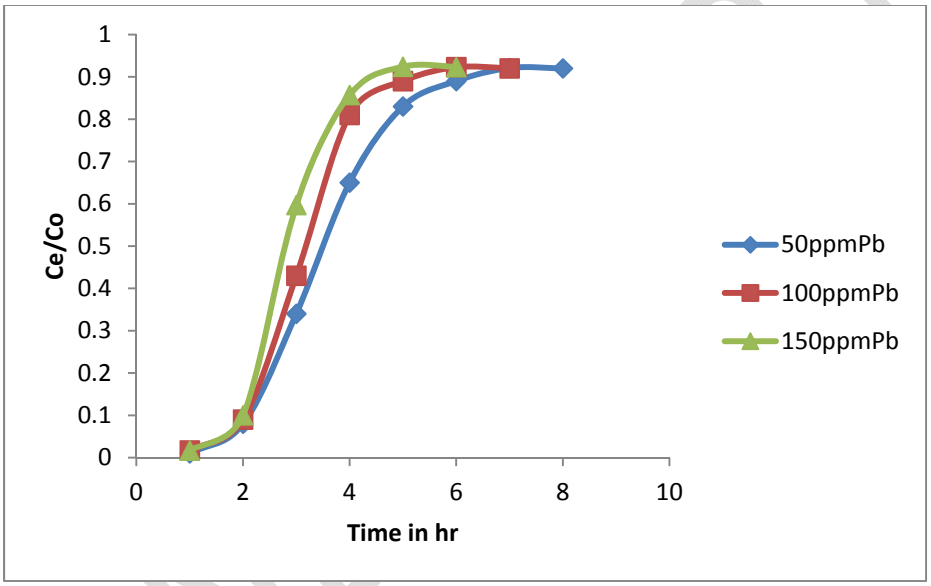

Figure 4.0: Column adsorption of Pb(II) by Activated Carbon from Velvet Tamarind Fruit shells at different Initial Concentration.

.

It can be seen from the Figure 4.0 that breakthrough curves display three important features: an initial lag period during which effluent metal ions are non-detectable, followed by a rise in concentration, and finally a period of slow increase in effluent level. It was assumed that the breakthrough metal-concentration would be 5% of the influent concentration. It is evident that by increasing initial metal concentration, the slope of the breakthrough curve increased and became much steeper, hence reducing the volume which can be treated before breakthrough occurred. This is due to the fact that by

increasing the initial metal concentration, the driving forces increases which enhance the rate of metal adsorption and saturates the binding sites more quickly. This is consistent with results of the finding of [35], where the authors found that by increasing inlet adsorbate concentration, the slope of the breakthrough curve increased and the volume treated before carbon regeneration reduced. This behaviour was attributed to the high concentrations which saturated the activated carbon more quickly, thereby decreasing the breakthrough time. It is also clear from Figures 1.0 to 5.0 that all the curves exhibit a characteristic "S" shape which indicates an effective use of adsorbent [36].

3.8.3 Effect of flow rate on breakthrough curves

The adsorption columns were operated with different flow rates (1, 3 and 5 cm^3/min) until no further metal ions removal was observed. The adsorbent bed height and inlet initial metal ions concentration were fixed at 10 cm and 50 mg/dm^3, respectively. The breakthrough curve for a column was determined by plotting the ratio of the Ce/C_0 (Ce and C_0 are the metal ions concentration of effluent and influent, respectively) against time, as shown in Figures 1.0 to 5.0 respectively. The effect of the flow rate on the adsorption of Cu, Cd, Pb and Ni are shown as breakthrough curves in the figures. It was observed that breakthrough generally occurred faster with higher flow rate. The reason is that at higher flow rate, the rate of mass transfer increased, thus the amount of metal ions adsorbed onto the unit bed height (mass transfer zone) increased [37]. In addition, the adsorption capacity decreases with increase in flow rates due to insufficient residence time of the solute in the column and lack of diffusion of the solute into the pores of the adsorbent, therefore the solute left the column before equilibrium occurred. These results were in agreement with other findings as reported by [38].

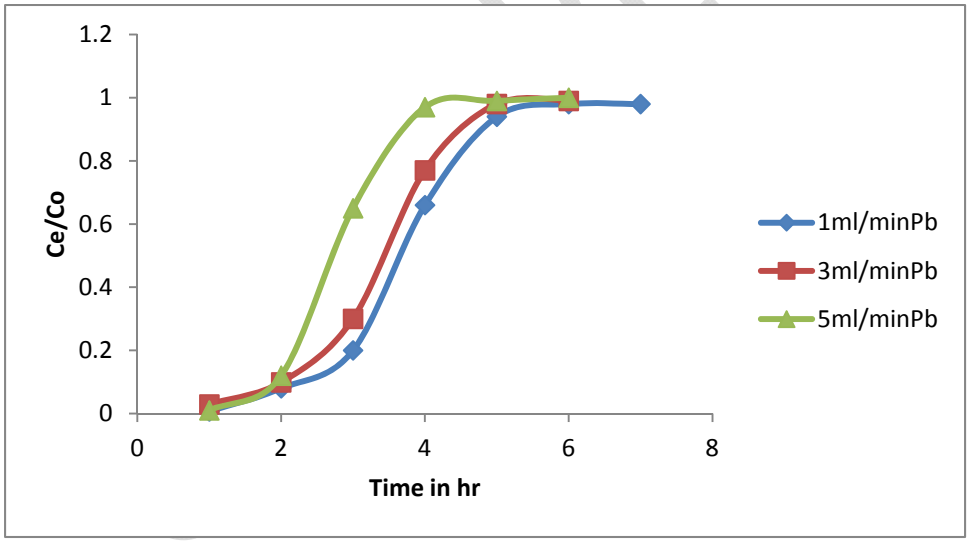

Figure 5.0: Column adsorption of Pb(II) by Activated Carbon from Velvet Tamarind Fruits Shell Activated Carbon at different Flow rate.

The column performed well at the lowest flow rate (1cm^3/min). Earlier breakthrough and exhaustion times were achieved, when the flow rate was increased from 1 to 5 cm^3/min. This was due to a decrease in the residence time, which restricted the contact of metal ions to the adsorbents. Similar results have been found for As (Ⅲ) removal in a fixed-bed system using modified calcined bauxite and for color removal in a fixed-bed column system using surfactant-modified zeolite [39].

3.9 Column Kinetic Study

Three models (Thomas model and Yoon-Nelson) were used to analyze the column performance.

3.9.1 Thomas model

The model was applied to the experimental data with respect to the initial metals concentration, flow rate and bed height. The kinetic coefficient, kTh and the adsorption capacity of the bed, q_o were determined from the plot of $\ln\left(\frac{Co}{Ce}-1\right)$against t The results of kTh, R^2 and q_o are given in Table 4.0. The results showed that the kinetic coefficient kTh is dependent on flow rate, initial ion concentration and bed height. The maximum adsorption capacity q_o and Kinetic coefficient kTh decreased with increase in flow rate but increased with increase in bed height and initial ion concentration. The values of kTh obtained in this work is similar to the ones obtained by [15]. High values of regression coefficients were obtained indicating that the kinetic data conformed well to Thomas model in contrast with the report of [40] but in agreement with the results obtained by [41]. The trend observed with the calculated values of kTh, q_o are in agreement.

3.9.2 Yoon and Nelson Model

This model is based on the assumption that the rate of decrease in the probability of adsorption for each adsorbate molecule is proportional to the probability of adsorbate adsorption and the probability of adsorbate breakthrough on the adsorbent [42]. The Yoon and Nelson equation for single component system is expressed as shown in equation 4.3 [43]:

$$ln\frac{Ce}{Co-Ce} = Kynt - \tau K \qquad (4.3)$$

Yoon and Nelson model has been used in the study of column adsorption kinetics [42][21]. The values of the Yoon-Nelson parameters (kyn and τ) were determined from the plot of $ln\frac{Ce}{Co-Ce}$ versus t at various operating conditions (Table 1.0 to 5.0). A plot of $ln\frac{Ce}{Co-Ce}$ versus t gives a straight line with slope of Kyn, and intercept of –τK. The results showed

that the rate constant, Kyn increased with increased inlet ions concentration, flow rate and bed height. The time required for 50% breakthrough, τ decreased with increase in flow rate and initial ion concentration. High values of correlation coefficients obtained indicate that Yoon and Nelson model fitted well to the experimental data and can be used to describe the Cd(II), Cu(II), Pb(II) and Ni(II)-Velvet Tamarind shell and Cd(II), Cu(II), Pb(II) and Ni(II) – Sandal fruit shell biosorption system.

355 **Table 4.0: Column kinetic parameters for Pb ions adsorption on activated carbon from Velvet tamarind fruit Shells**

	Initial ion concentration(mg/dm^3)			Flow rates in cm^3/min			Bed height (cm)		
	50	100	150	1	3	5	5	10	15
Thomas									
K_{Th} (cm^3/min/mg)									
X10^{-3}	2.40	7.20	2.30	0. 34	0. 38	0. 64	0. 24	0. 42	0. 42
q_o (mg/g)	1.20	1.93	2.80	0.71	0.38	2.10	1.00	1.20	1.80
R^2	0.98	0.97	0.95	0.98	0.99	0.98	0.96	0.95	0.99
Yoon & Nelson									
Kyn (min^{-1})	1.00	1.40	2.00	1.60	2.00	2.50	1.90	1.90	3.10
X10^{-2}									
ĭ (min)	251.00	205.00	125.00	173.00	167.00	126.00	125.00	150.00	194.00
R^2	0.95	0.99	0.94	0.97	0.99	0.94	0.97	0.99	0.97

356

3.9.3 Lead Uptake in the Column at Different Operating Parameters

This study showed that the sorption uptake capacity of the column Pb 1.73 mg g^{-1} for velvet tamarind fruit shells activated carbon as shown in Table 5.0. The increased capacity of the column method is largely due to the continuous increased concentration gradient in the interface of the adsorption zone as it passes through the column, whereas the gradient concentration decreases with time in batch systems [44][45]

A characterisation study on the Velvet Tamarind shells prior to biosorption showed that hydroxyl and carboxylic functional groups were present and might be involved in the removal of metal ions from aqueous solutions by this biosorbent, besides micro precipitation and electrostatic attraction forces. The results obtained by [44] for Ni(II), Cd(II), Zn(II) and Pb(II) ions using H_2SO_4 treated coconut shell suggest that a lower pH of 6 is required for optimal removal of the studied metals, similar to the pH of 6 ± 0.2 used in this study.

Table 5.0: Uptake of PbII) by activated carbon from Velvet Tamarind Fruit shells at different flow rates

	Z (cm)	Q (cm^3min^{-1})	C_0 (mg $dm^{-3)}$)	V_{eff} (cm^3)	q_{total} (mg)	$qe_{(exp)}$ (mgg^{-1})	Zm (cm)
Vt	10.00	1.00	50.00	1191.00	1.79	1.73	6.40
	10.00	3.00	50.00	882.00	0.44	1.64	7.95
	10.00	5.00	50.00	300.00	0.30	0.54	5.50

4.0 Conclusion

i. The experimental data revealed that an increase in bed height and initial metal concentration or a decrease of flow rate enhances the longevity of column performance by increasing both breakthrough time and exhaustion time thereby delaying bed saturation.

ii. The design of a continuous fixed bed column for removal of metal ions by velvet tamarind and sandal fruit shells activated carbons can be achieved using the BDST, Yoon-Nelson and Thomas models.

iii. The FTIR analysis results suggested the presence of functional groups such as hydroxyl, carbonyl, carboxyl and amine which could bind the metals and remove them from the solution.

iv. The values of moisture content, volatile matter, fixed carbon and ash content as obtained from % proximate analysis are 3.43, 27.07, 65.05, 4.45 for activated carbons prepared from velvet tamarind shells.

v. Ultimate analysis revealed that activated carbons prepared from velvet tamarind shells contained 75% carbon.

5.0 REFERENCES

Oliveira, R. C., Guibal, E. & Garcia, O. (2012). Biosorption and desorption of lanthanum (III) and neodymium(III) in fixed-bed columns with Sargassum sp. Perspectives for separation of rare earth metals. *Biotechnology Progress*, 28(3), 715-722.

Ahluwalia, S. S., & Goyal, D. (2005). Removal of heavy metals by waste tea leaves from aqueous solution. *Engineering and Life Science,* 5(9),158- 162.

Nouri, J., Mahvi, A. H., Babaei, A. A., Jahed, G. R., & Ahmadpour, E. (2006). Investigation of heavy metals in groundwater *Pakistan Journal of Biologial Science,* 9 (3), 377-384

Dermibas, A. (2008). Heavy metal adsorption onto agro-based waste materials: A review*. Journal of Hazardous Material,* 157(8), 220-229

Lazaridis, N. K., Matis, K. A., & Diels, L. (2005). 'Application of flotation to the solid/liquid separation of *Ralstonia metallidurans*', *3rd Eur. Bioremediation Conf.*, TU Crete, Chania,4–7 July.

Kuma, A., & Jena, H.M (2015) Applied Surface Science 356: 753–761.

Abia, A. A., & Asuquo, E. D. (2007). Kinetics of Cd^{2+} and $Cr+^{3+}$ Sorption from aqueous solution using mercaptoacetic acid modified and unmodified oil palm fruit fibre (*elaeis*

Sing, K. S. W., Everett, D. H., Haul, R. A. W., Moscou, L., Pierotti, R. A., Rouquerol, J., & Siemieniewska, T. (2006). Reporting Physisorption data for gas/solid interface with special reference to the determination of surface area and porosity. *Pure and Applied Chemistry*. 57, 603-619.

Kahraman, S., Dogan, N., & Erdemoglu, S. (2008). Use of various agricultural wastes for the removal of heavy metal ions. *International Journal of Environmental Pollution,* 34, 275-284.

American Society for Testing and Materials. (1996). Standard, Refractories, Carbon and Graphic Products; activated Carbon, ASTM, Philadelphia, PA, 15(01)

Ahmedna, M., Johns, M. M., Clarke, S. J., Marshall, W. E., & Rao, R. M. (1997). Potential of agricutural by-product-based activated carbons for use in raw sugar decolourisation. *Journal of the Science of Food and Agriculture*, 7(5),117-124.

American Society for Testing and Materials. (1986). Standard test method for determination of iodine number of activated carbon. Philadelphia, PA: ASTM Committee on Standards.

Al-Quodah, Z., & Shawabkah, R. (2009). Production and characterization of granular activated carbon from activated sludge. *Brazilian Journal of Chemical Engineering*, 26(1), 6-10.

Alam, C., Molina-Sabio, M., & Rodriguez-Reinoso, F. (2008). Adsorption of methane into $ZnCl_2$-activated carbon derived discs. *Microporous and Mesoporous Materials*, 76(15), 185-191

Yahaya, N. K. E. M., Abustana, I., Latiff, M. F. I. P. M., Bello, O. S. & Ahmad, M. A. (2011). Fixed-bed column study for Cu (II) removal from aqueous solutions using rice *hu*sk based activated carbon. *International Journal of Engineering & Technology*, 11(1), 248-252.

Maheswari, B. L., Mizon, K. J., Palmer, J. M., Korsch, M. J., Taylor, A.J., & Mahaffey, K.R. (2008). Blood lead changes during pregnancy and postpartum with calcium supplementation. *Environmental Health Perspectives,* 112(15), 1499-1507.

Mozammel, H. M., Masahiro, O., & Bhattacharya, S. C. (2010). Activated charcoal from coconut shell using $ZnCl_2$ activation. *Biomass and Bioenergy*, 22(6), 397-400.

Gottipati, R., & Susmita, M.(2012). Process optimization of adsorption of Cr(VI) on activated carbons prepared from plant precursors by a two-level full factorial design. *Chemical Engineering Journal*, 160 (1), 99-107.

Pandey, K. K., Prasad, G., & Singh, V. N. (2014). Use of wollastonite for the treatment of Cu(II) rich effluent. *Water Air and Soil Pollution,* 27, 287-296.

Valix, M., Cheung, W. H., & McKay, G. (2004). Preparation of activated carbon using low temperature carbonization and physical activation of high ash raw bagasse for acid dye adsorption. *Chemosphere*, 56, 493-501

Satyawali, Y., & Balakrishnan, M. (2009). Wastewater treatment in molasses-based alcohol distilleries for COD and color removal: A review. *Journal of Environmental Management,* 86, 481-497.

Lopez, F. A., Perez, C., Sainz, E., & Alonso, M. (1995). Adsorption of Pb (II) on blast furnace sludge*, Journal of Chemical Technology*., 62 (2), 200-206.

Kanan, K., & Sundaram, M. M. (2001). "Kinetics and mechanism of removal of methylene blue by adsorption on various carbons—a comparative study", *Dyes and Pigments*. 51, 25–40.

Karthikeyan, S., Balasubramanian, R., & Iyer, C. S. P. (2008). Evaluation of the marine algae *Ulva fasciata* and *Sargassum* species for the biosorption of Cu(II) from aqueous solutions. *Bioresource Technology*, 98 (2), 452-455.

Vijayaraghavan, K., Padmesh, T. V. N., Palanivelu, K., & Velan, M. (2006). Biosorption of nickel(II) ions onto Sargassum wightii: Application of two-parameter and three-parameter isotherm models. *Journal of Hazardous Materials,* 133, 304-308.

Mohammed, U. M., Binta, M., Mustapha, S., & Idris, M (2016) Removal of Lead and Cobalt from Pharmaceutical Effluent: Efficiency of Activated Coconut Shell and Commercial Activated Carbon. *American Chemical Science Journal,* 12(2), 1-8

Alikarami, M., Abbari, Z., & Mohammadnezhad, S. (2016). Kinetics and thermodynamic studies of copper (II), mercury(II) and chromium(II) adsorption from aqueous solution by peels of banana. *Journal of Basic and Applied Scientific Research,* 3(3), 8-15.

Amuda, O. S., Giwa, A. A., & Bello, I. A. (2007). Removal of heavy metal from industrial wastewater using modified activated coconut shell carbon. *Biochemical Engineering Journal,* 36(23), 174-181.

Deheyn, D. D., Gendreu, P., Baldwin, R. J., & Latz, M. I. (2005). Evidence for enhanced bioavailability of trace elements in the marine ecosystem of Deception Island, a volcano in Antarctica. *Marine Environmental Research,* 60(4), 1-33.

Castro, A., Suarez-Garcia, F., Martinez-Alonso, A., & Tascon, J. M. D. (2008). Activated carbon fibers with a high content of surface functional groups by phosphoric acid activation of PPTA. *Journal of Colloid and Interface Science*, 3(61), 307-315.

Liu, S., & Liu, J. (2008). Surface modification of coconut shell based activated carbon for the improvement of hydrophobic VOC removal. *Journal of Hazardous Materials*, 192 (2), 683-690.

Yang, X., & Duri, B. A. (2005). "Kinetic modeling of liquid-phase adsorption of reactive dyes on activated carbon". *Journal of Colloid Interface Sciences*, 287, 25-34.

Alothman, Z.A., Habila, M.A & Ali, R. (2011). Preparation of activated carbon using the copyrolysis of agricultural and municipal solid wastes at a low carbonization temperature. In: Proceedings of the international conference on biological and environmental chemistry: 24, 67–72

Betzy, N. T., & Soney., C .(2015). Cyanide in industrial wastewaters and its removal: A review on biotreatment. *Journal of Hazardous Materials,* 163, 1-11

Tamura, H., Hamaguchi, T., & Tokura, S. (2003). "Destruction of rigid crystalline structure to prepare chitin solution", *Advances in chitin science.* 7, 84–87.

Patil, S., Bhole, A., & Natrajan, G. (2006). Scavenging of Ni(II) Metal Ions by Adsorption on PAC and Babhul Bark. *Journal of Environmental Science and Engineering,* 48(3), 203-208.

Volesky, B. (2005). Advances in biosorption of metals: selection of biomass types. *Microbiology Reviews*, 14, 291–302.

Hrapovic, L., & Rowe, R. K. (2002). Intrinsic degradation of volatile fatty acids in laboratory- compacted clayey soil. *Journal of Contaminant Hydrology*, 58, 221- 242

Sasikala, S., &. Muthuraman, G. (2016) Removal of Heavy Metals from Wastewater Using *Tribulus terrestris* Herbal Plants Powder. *Iranica Journal of Energy and Environment,* 7(1),39-47.

Baek, K., Song, S., Kang, S., Rhee, Y., Lee, C., Lee, B., Hudson, S., & Hwang, T. (2007). Adsorption kinetics of boron by anion exchange resin in packed column bed. *Journal of Industrial Engineering Chemistry,* 13(3), 452-456.

Kavak, D., & Öztürk, N. (2004). Adsorption of boron from aqueous solution by sepirolite: II. Column studies. II. Illuslrararasi. *Journal of American Chemical Society*, 23(25), 495-500.

Aksu, Z., Gönen, F., & Demircan Z. (2004). Biosorption of chromium (VI) ions by Mowital®B30H resin immobilized activated sludge in a packed bed: comparison with granular activated carbon. *Process Biochemistry*, 38(2),175-186

Sousa, F. W. (2010). Green coconut shells applied as adsorbent for removal of toxic metal ions using fixed-bed column technology. *Journal of Environmental Management*, 91(8), 1634-1640

Martín-Lara, M. A., Blázquez, G., Ronda, A., Rodríguez, I.L., & Calero, M. (2012). Multiple biosorption–desorption cycles in a fixed-bed column for Pb(II) removal by acid-treated olive stone. *Journal of Industrial and Engineering Chemistry*, 18(3), 1006-1012